

Supplementary Information

Investigating the origin of high efficiency in confined multienzyme catalysis

Yufei Cao^{1†}, Xiaoyang Li^{1†}, Jiarong Xiong¹, Licheng Wang¹, Li-Tang Yan^{2*}, Jun Ge^{1*}

1 Key Lab for Industrial Biocatalysis, Ministry of Education, Department of Chemical Engineering, Tsinghua University, Beijing 100084, China

2 State Key Laboratory of Chemical Engineering, Department of Chemical Engineering, Tsinghua University, Beijing 100084, China

†These authors contributed equally to this work.

*Email: junge@mail.tsinghua.edu.cn; ltyan@mail.tsinghua.edu.cn

Content

1. Supplementary Figure S1	page 3
2. Supplementary Figure S2	page 4
3. Supplementary Figure S3	page 5
4. Supplementary Figure S4	page 6
5. Supplementary Figure S5	page 7
6. Supplementary Figure S6	page 8
7. Supplementary Figure S7	page 9
8. Supplementary Figure S8	page 10
9. Supplementary Figure S9	page 11
10. Supplementary Figure S10	page 12
11. Supplementary Figure S11	page 13
12. Supplementary Figure S12	page 14
13. Supplementary Figure S13	page 15
14. Supplementary Figure S14	page 15
15. Simulation details of cascade reaction in bi-enzyme system	page 16
16. Coarse-grained details of simulation model	page
16	
17. Simulation of steady-state reaction of enzyme cluster	page 17
18. Supplementary Figure S15	page 17
19. Supplementary Figure S16	page 18
20. Derivation process of probability of intermediate decay	page 18
21. Estimation of the distance between enzyme molecules in ZIF-8	page 19
22. Supplementary Figure S17	page 20
23. Materials	page
20	
24. Characterizations	page 20
25. Activity assay of GOx/HRP@ZIF-8 composite	page 21
26. Preparation of fluorescently labeled GOx/HRP@ZIF-8 composite	page 21

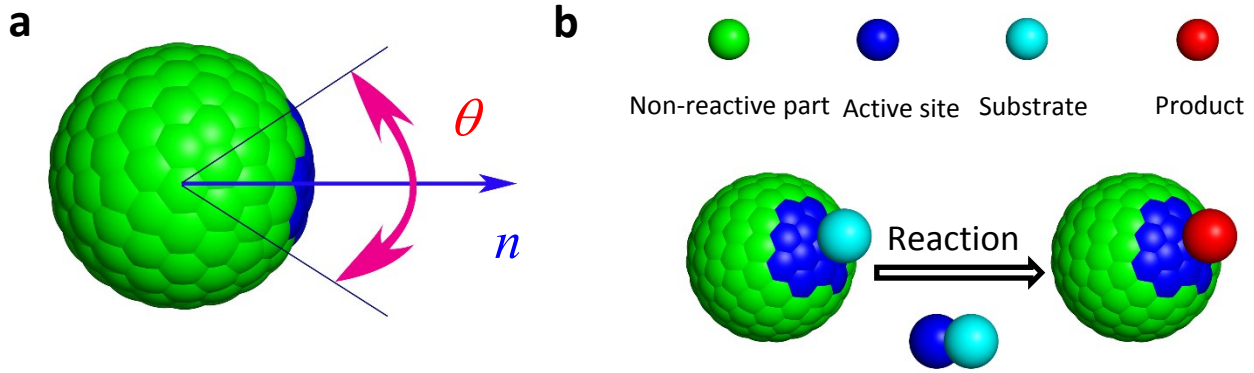


Figure S1. Detailed definitions of the model we developed. (a) We used θ and n to describe the size and orientation of active site. In our simulation, θ was set to $\pi/3$ and the orientation was random. The ratio of area of active site surface could be calculated as follows:

$$S(\text{active site}) / S(\text{all}) = \int_0^{\pi/6} \sin\theta d\theta / \int_0^{\pi} \sin\theta d\theta = \frac{2-\sqrt{3}}{4} \approx 0.067.$$

Therefore the area of active site surface was approximately 6.7% of the total surface area of the enzyme sphere.

(b) We used the following criteria to judge the occurrence of the reaction: when a substrate (cyan sphere) met the active site of enzyme (blue sphere), the reaction took place with 3/10 probability if the distance between substrate and active site particle is less than 0.8σ . (σ is the unit length in DPD simulation, which is equal to the diameter of a substrate sphere).

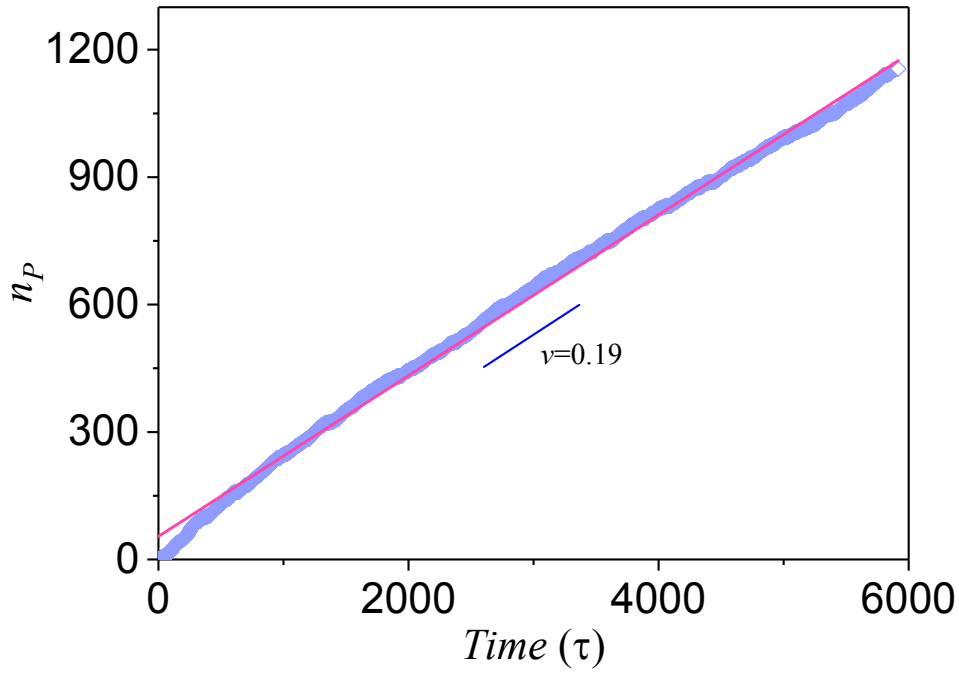


Figure S2. The method used to obtain the steady state reaction rate, v . We place one enzyme molecule in a $30 \times 30 \times 30$ simulation box (number of DPD particles was $30^3 \times 3 = 81000$) with different concentrations of substrates. When the reaction reached its steady state, we calculated the reaction rate, v (molecular/ τ) by fitting the curve of reaction products number, n_p over time. The slope of fitting line stands for the reaction rate, v . The figure showed that the number of substrate particles was 3000. Therefore the concentration of substrate C_S was $N_{substrate}/N = 3000/81000 = 0.0370$, $N_{substrate}$ was the number of substrate particles and N was the number of substrate and water particles. According to fitting results, we can estimate the steady state reaction rate, v under conditions $C_S = 0.0370$, $v = 0.19$ molecular/ τ .

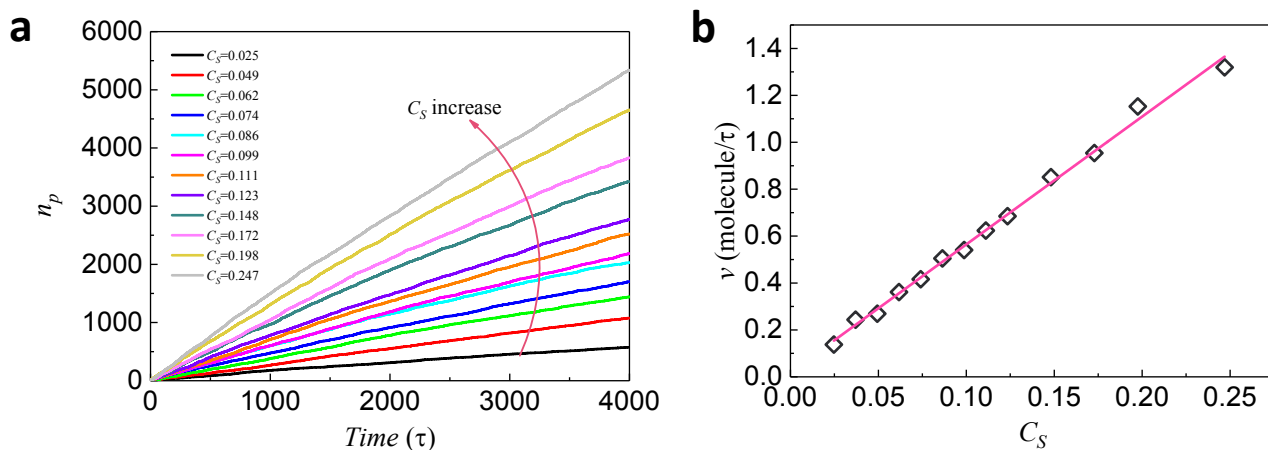


Figure S3. The reaction kinetics of single enzyme without restriction of turnover number. (a) We calculated the reaction rate under different substrate concentrations C_s (from 0.025 to 0.247). Through fitting lines, we can obtain steady state reaction rates, ν in all cases. **(b)** The steady state reaction rate of single enzyme versus concentration of substrate. As shown in the figure, ν increased linearly with the increasing concentration of the substrate, though the concentration of substrate was sufficiently large.

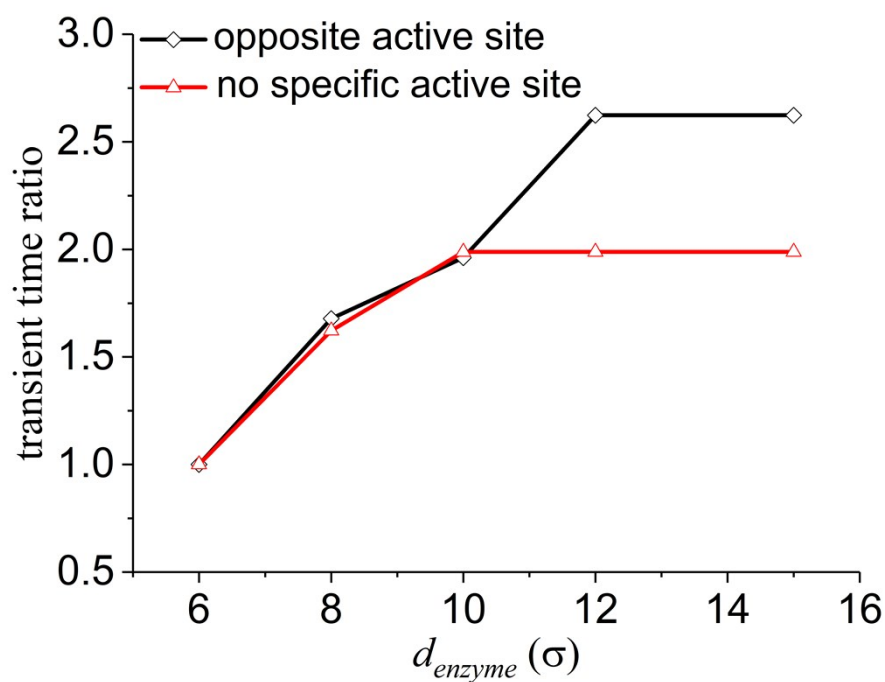


Figure S4. The substrate channeling effect with varied d_{enzyme} under two conditions: active part only and two enzymes with opposite orientation of active sites. Here we used the ratio of transient time to indicate the dependence of substrate channeling effect on d_{enzyme} . The transient time ratio was defined as the ratio of transient time to transient time under $d_{enzyme}=6$. The effect of substrate channeling could be more clearly observed in the case of opposite active sites.

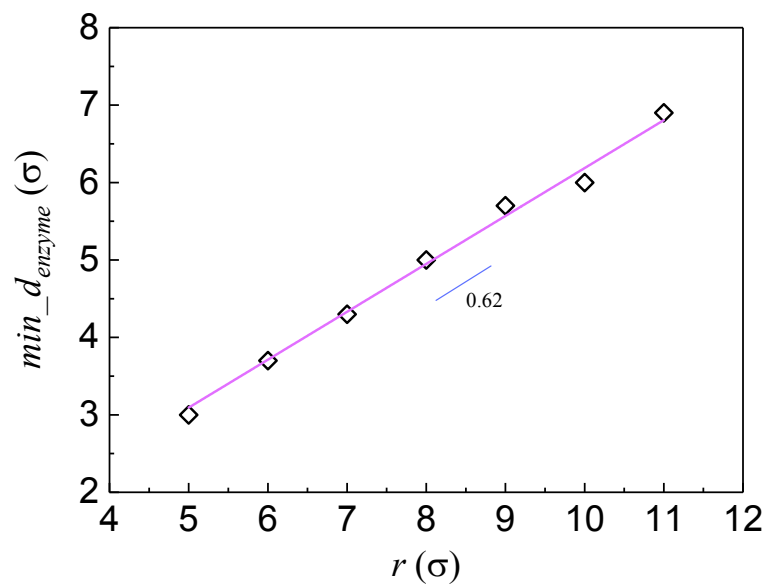


Figure S5. The minimum distance of enzymes, min_d_{enzyme} , when 20 enzyme molecules were evenly distributed in a spherical area representing an enzyme cluster with different radiuses, r . The minimum distance between enzymes, min_d_{enzyme} , increased linearly with r .

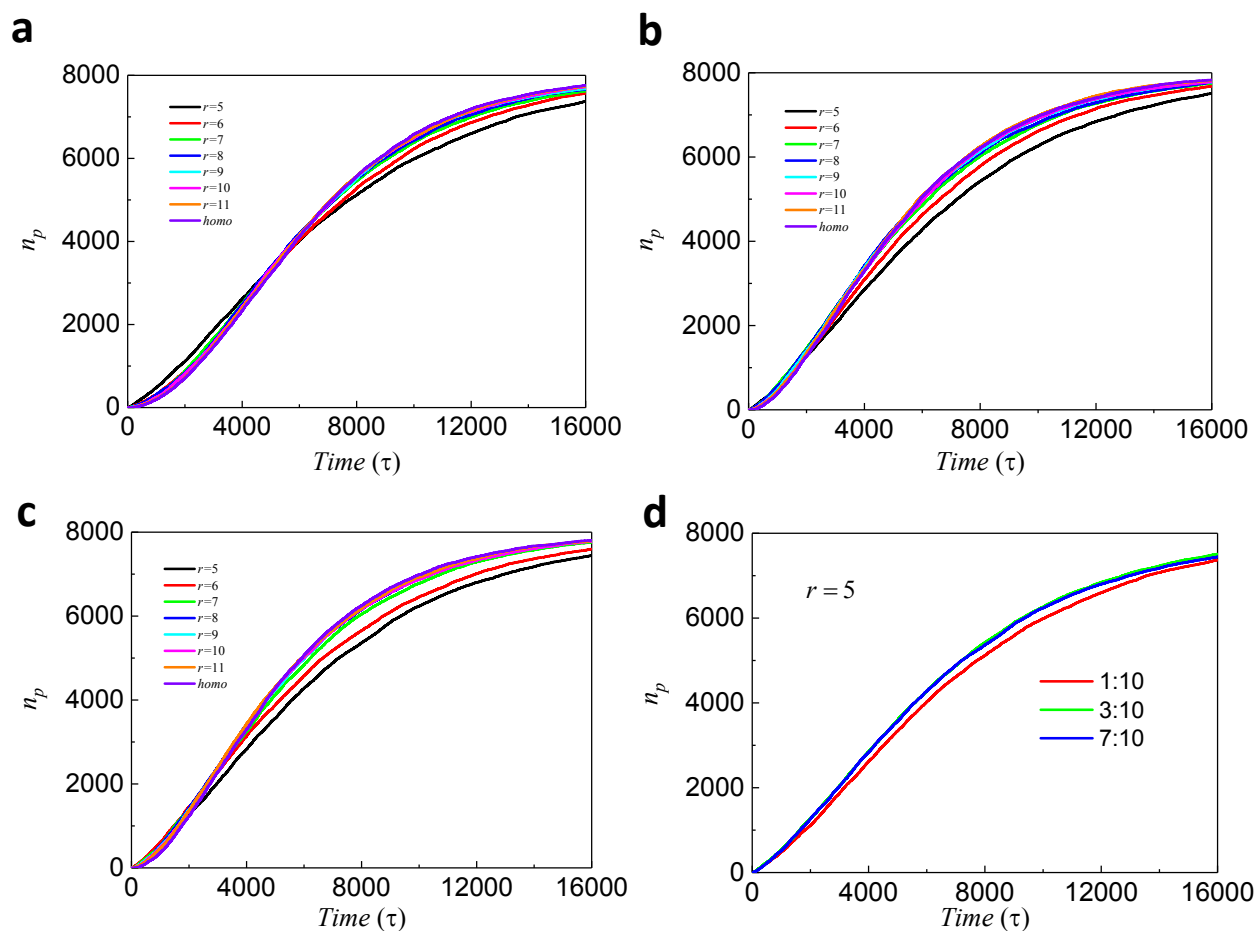


Figure S6. Cascade reaction of enzyme clusters without intermediate decay under different turnover number ratios of E_1 to E_2 . The ratios of Figure (a), (b) and (c) are 1:10, 3:10 and 7:10, respectively. Notably, the smaller turnover number ratio of E_1 to E_2 resulted in more significant impact on distance in early stage of reaction. Therefore, we set a smaller turnover number ratio to observe the remarkable effect of radius of spherical enzyme clusters on the substrate channeling. Figure (d) gave the reaction kinetics (number of product, n_p , versus simulation time) of three ratios at $r=5$.

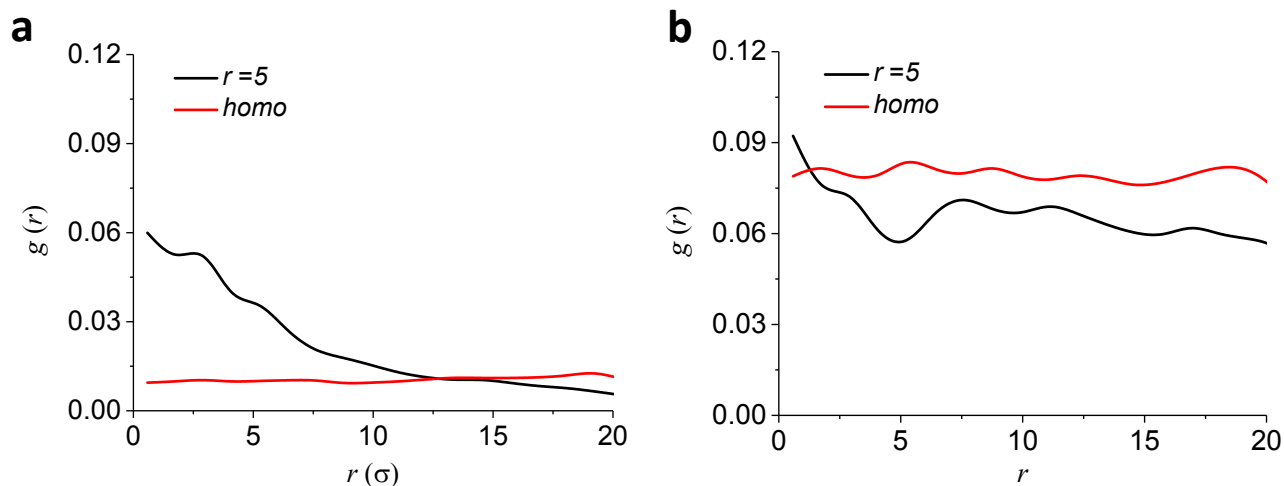


Figure S7. Radial distribution function, $g(r)$ of intermediate S_I relative to the center of the simulation box.

$g(r)$ can be used to characterize the concentration distribution of S_I in the simulation box. The radial distribution function $g(r)$ can reflect the probability of finding an intermediate product when the distance from the center of the box is r . The size of the box was $40 \times 40 \times 40$ (σ) **(a)** $g(r)$ of S_I at 800τ . The intermediates mainly distributed inside and nearby the enzyme cluster at $r=5$, as they distributed uniformly throughout the box in “homo”. **(b)** $g(r)$ of S_I at 6600τ . The intermediates distributed uniformly throughout the box in both cases, as the concentration of intermediates in “homo” was relatively higher.

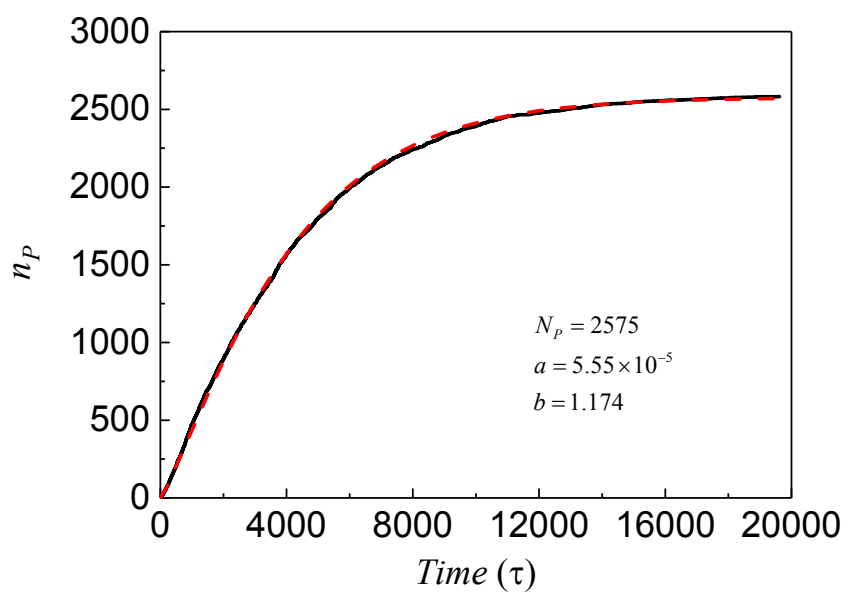


Figure S8. The fitting of reaction kinetics curve. We fitted the curve of number of product, n_p , versus simulation time (take $r=5$ as an example) to get parameters: a and b . The fitting curve (red dotted line) fitted well with the original curve (black solid line).

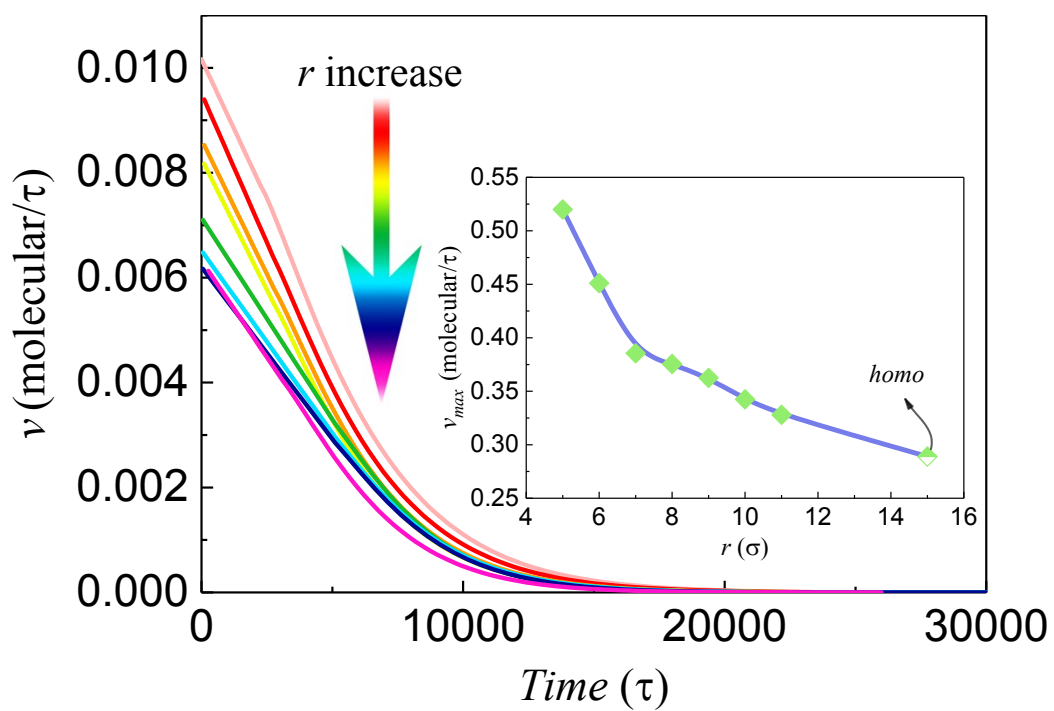


Figure S9. Reaction rate, v , versus simulation time. We can derive the reaction rate from the fitted product-time curve. Inset: the maximum reaction rate, v_{max} , versus radius of enzyme clusters, r .

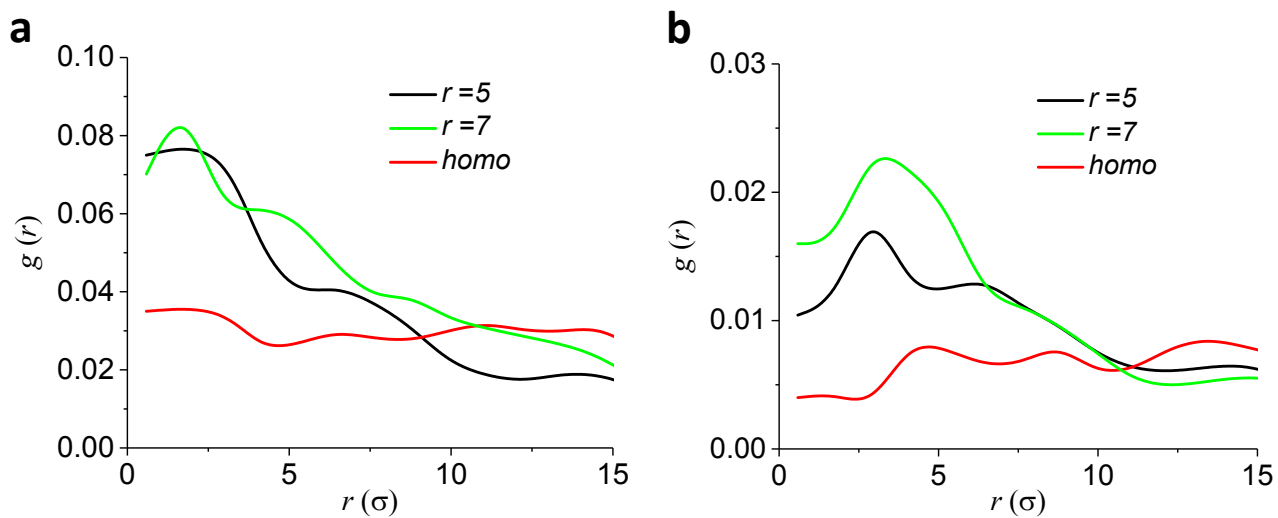


Figure S10. Radial distribution function, $g(r)$ of intermediate S_I . $g(r)$ was used to characterize the concentration distribution of S_I in the $40 \times 40 \times 40(\sigma)$ simulation box. **(a)** $g(r)$ of S_I at 800τ . **(b)** $g(r)$ of S_I at 6600τ . Enrichment of intermediates can be observed in both cases, $r=5$ and $r=7$. This advantage still maintained recognizable at the middle-late stage of the reaction.

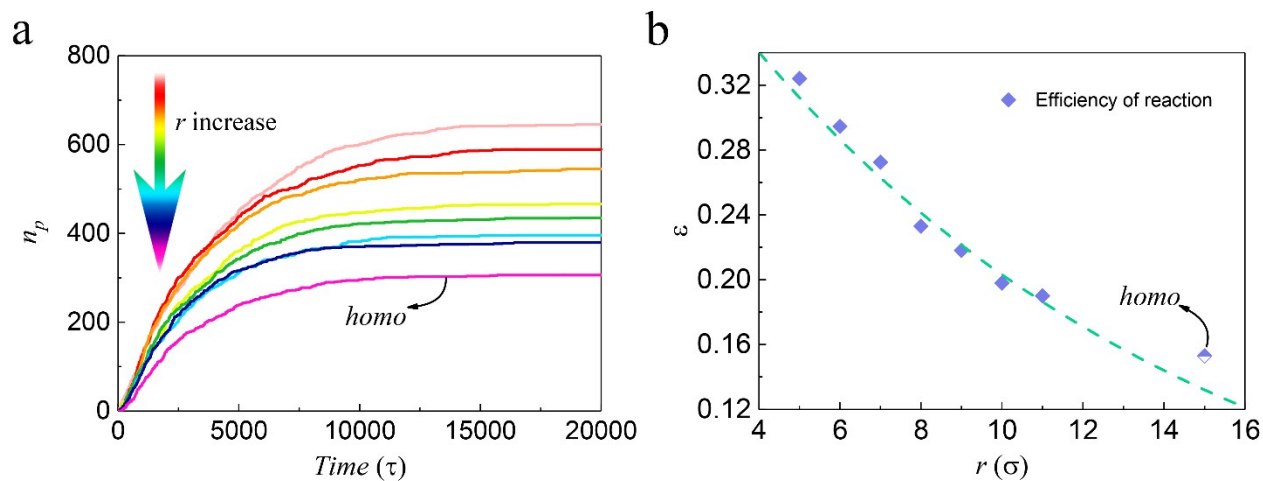


Fig. S11. Cascade reaction at lower substrate concentration catalyzed by the enzyme cluster. Enzyme cluster was located in a $30 \times 30 \times 30(\sigma)$ cubic box and parameter of decay probability of S_j : $\beta = 1 \times 10^{-7} \tau^{-1}$. The initial concentration of substrate was 0.12 mol/L (number of substrate beads is 2000, $C_S = 0.0247$) (a) Reaction kinetics with intermediate decay (number of products, n_p , versus simulation time) for different radius of enzyme clusters, $r = 5, 6, 7, 8, 9, 10, 11(\sigma)$ and “homo”. The direction of the arrow indicates the increase of radius r . (b) Yield of reaction, ϵ , versus radius of enzyme clusters, r . The dashed line represented the fitting curve with the expression: $\epsilon \sim \exp(-kr)$, $k = 0.086$.

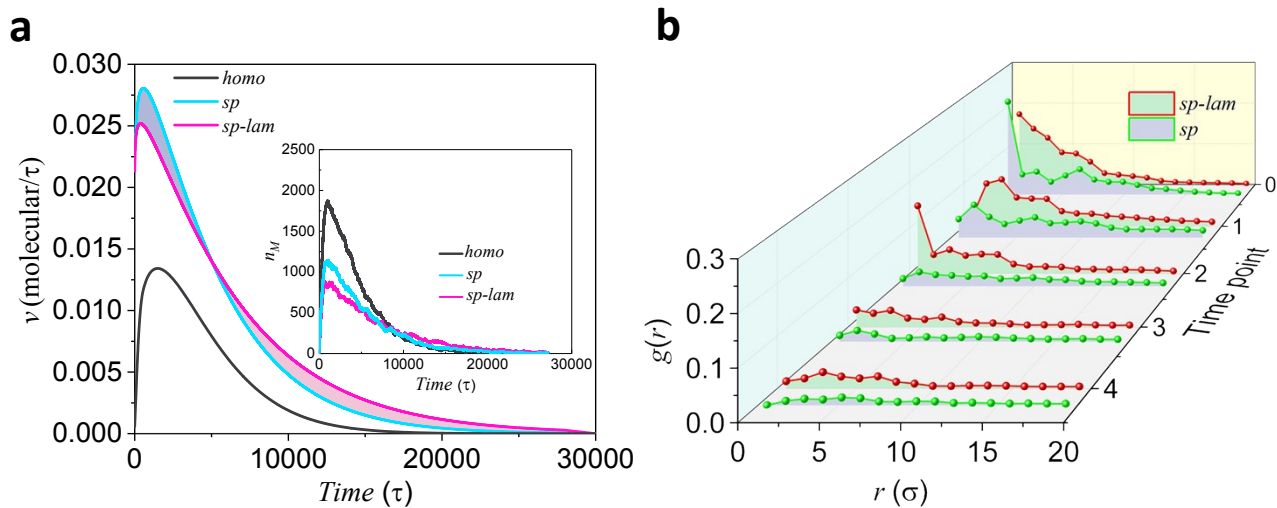


Figure S12. The effect of compartmentalized structures of enzyme clusters on cascade reaction kinetics with intermediate decay. The size of simulation box was $40 \times 40 \times 40(\sigma)$. **(a)** Reaction rate, ν , versus simulation time of three enzyme structures with intermediate decay. Inset: number of intermediate, n_M , versus simulation time. **(b)** The radial distribution function of structure *sp-lam* and *sp*. Data were collected at five time points, 300τ , 1260τ , 5680τ , 8780τ and 9640τ .

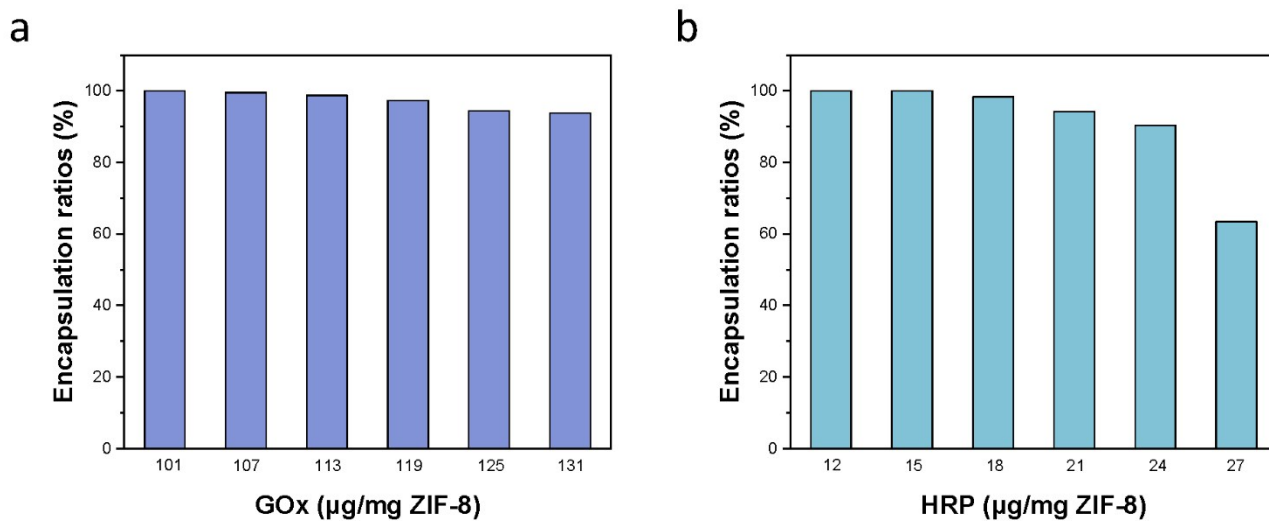


Figure S13. Encapsulation ratios of GOx and HRP in ZIF-8 at different inputs of enzymes. To obtain 100% encapsulation ratios, the maximum amounts of GOx and HRP were 101 and 15 μg per milligram ZIF-8, respectively.

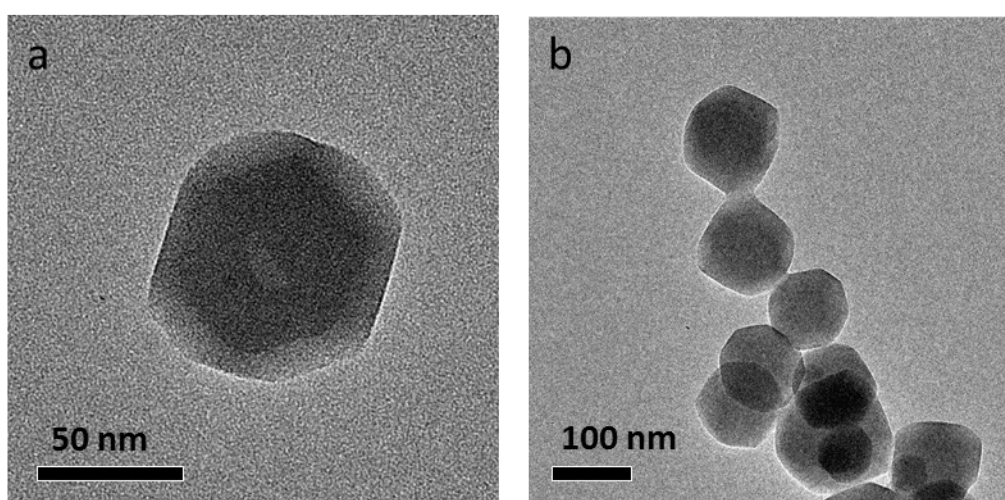


Fig. S14. The representative TEM images of GOx/HRP@ZIF-8 composites.

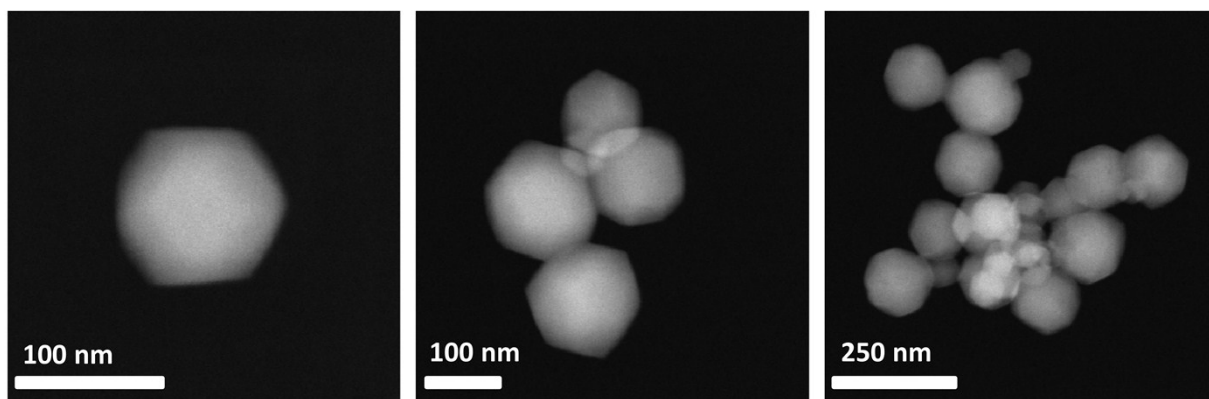


Figure S15. HAADF-STEM images of GOx/HRP@ZIF-8 composites.

Simulation details of cascade reaction in bi-enzyme system



As shown in formula S-2, the reaction was first catalyzed by enzyme E_1 , turning the substrate S_0 into intermediate S_1 , which was then catalyzed by enzyme E_2 to product P . In all cascade reaction simulations, two enzymes E_1 and E_2 are fixed in the simulation box of $30 \times 30 \times 30$ (σ) filled with water and substrate. The criteria to judge the occurrence of the reaction was given in **Supplementary Fig. S1**. We investigated the substrate channeling effects in the cases of the bi-enzyme systems without specific active sites, with active sites opposite in orientation, and active sites same in orientation. The distance between the centers of two enzyme spheres d_{enzyme} varied as 6, 8, 10, 12, 15(σ).

Coarse-grained details of simulation model

Reduced units were used in our simulations. The dimensionless temperature T , length L and mass m are scaled from their physical counterparts T^* , L^* and m . They can be obtained by scaling as follows:

$$T \text{ B} \frac{T^*}{T_0} = \frac{T^*}{298.15 \text{ K}}, \quad L \text{ B} \frac{L^*}{\sigma} = \frac{L^*}{1 \text{ nm}}, \quad m \text{ B} \frac{m^*}{m_0} = \frac{m^*}{200 \text{ Da}} \quad (\text{S-1})$$

L_0 , in our simulation, is set to 3 σ , referring to the diameter of enzyme molecule is generally within a few nanometers. m_0 is referring to the density of water and DPD particle number density $\rho_n = 3$. Each solvent bead represents 11 water molecules and each substrate bead represents a substrate molecule. (molecular weight of substrate is generally several times that of water. For example, the molecular weight of glucose is 10 times of water.)

According to the above scaling process, we can calculate the physical counterparts of substrate and enzyme concentrations. In our simulation, 8000 or 20000 substrate beads were put in box of $30 \times 30 \times 30$ (σ) or $40 \times 40 \times 40$ (σ).

The concentration of substrate is calculated as following:

$$c_S(30) = \frac{8000 / 6.02 \times 10^{23} \text{ mol}}{(30 \times 10^{-8})^3 \text{ L}} = 0.49 \text{ mol / L}$$

$$c_S(40) = \frac{20000 / 6.02 \times 10^{23} \text{ mol}}{(40 \times 10^{-8})^3 \text{ L}} = 0.52 \text{ mol / L}$$

Concentration of enzyme E_1 and E_2 :

$$c_E(30) = \frac{20 / 6.02 \times 10^{23} \text{ mol}}{(30 \times 10^{-8})^3 \text{ L}} = 1.23 \times 10^{-3} \text{ mol / L}$$

$$c_E(40) = \frac{20 / 6.02 \times 10^{23} \text{ mol}}{(40 \times 10^{-8})^3 \text{ L}} = 5.2 \times 10^{-4} \text{ mol / L}$$

Simulation of steady-state reaction catalyzed by enzyme cluster

As NVT ensemble was used to simulate enzyme reaction, steady-state reaction simulation cannot be carried out straightforwardly. Herein we ensured a constant substrate concentration by replacing water beads outside the enzyme cluster with substrate beads. As a_{ij} between different beads i and j is the same, this trick has no influence on the physical properties of the system. And the number of solvent beads is much higher than the number of substrate beads. The results of this steady-state cascade reaction showed that the effect of radius of enzyme clusters, r on the reaction rate, is significantly different from an unsteady-state reaction. With r increasing, the steady reaction rate increases and finally reaches a constant value regardless of the decay of intermediates.

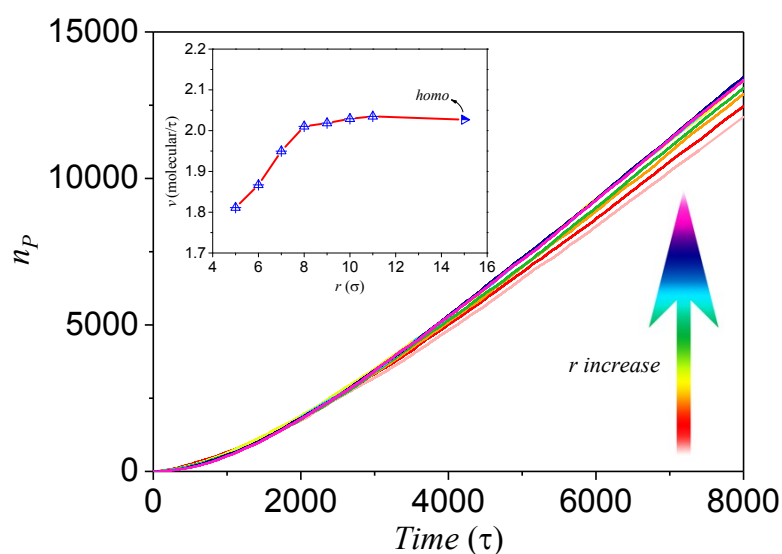


Figure S16. Results of steady-state cascade reaction without intermediate decay. Enzyme cluster in a $40 \times 40 \times 40(\sigma)$ cubic box and the substrate concentration stayed constant at 0.13 mol/L (number of substrate beads is 5000, $C_S = 0.026$). Reaction kinetics (number of products, n_p , versus simulation time) of different radius of enzyme clusters, $r=5, 6, 7, 8, 9, 10, 11(\sigma)$. The direction of the arrow indicated the increase of distance r . Inset: steady-state reaction rates of different sizes of enzyme cluster.

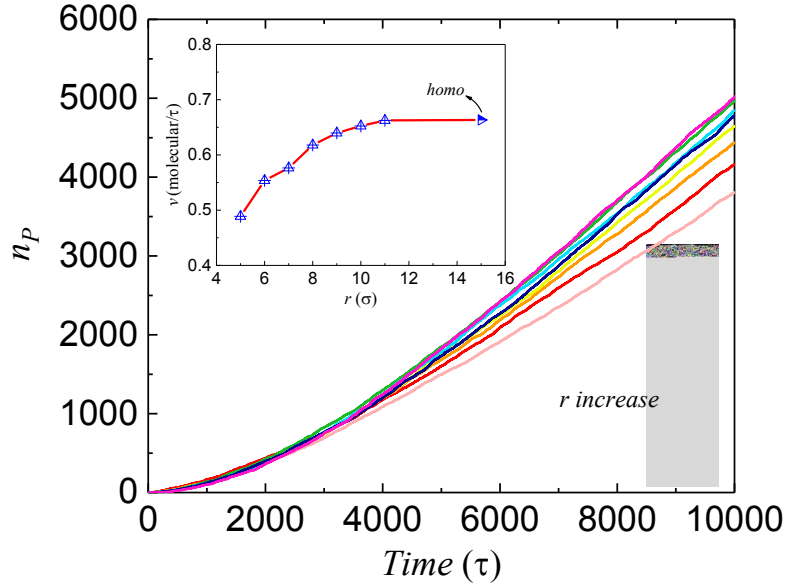


Figure S17. Results of steady-state cascade reaction with intermediate decay. Enzyme cluster in a $30 \times 30 \times 30(\sigma)$ cubic box and the substrate concentration was constant at 0.12 mol/L (number of substrate beads is 2000, $C_S = 0.026$). Parameter of decay probability of $S_I \beta$ is set to $1 \times 10^{-7} \tau^{-1}$. Reaction kinetics (number of products, n_p , versus simulation time) of different radius of enzyme clusters, $r=5, 6, 7, 8, 9, 10, 11(\sigma)$. The direction of the arrow indicated the increase of distance r . Inset: Reaction rate at which the reaction reaches steady state.

Derivation process of probability of intermediate decay

We assumed that the kinetic equation of the decay process of the intermediate could be expressed by the equation below:

$$\frac{dc_1}{dt} = -\beta c_1 \quad (\text{S-2})$$

Where c_1 is concentration of intermediates and β indicates the rate of intermediate decay. Considering the kinetic equation of intermediate decay in this form is extensive in the study of enzyme cascade reactions. c_1 can be calculated as follows: $c_1 = N_1/V$, where N_1 and V are number of intermediates and volume of simulation box, respectively. The above formula is converted into the following form:

$$\frac{dN_1/V}{dt} = -\beta N_1/V \quad (\text{S-3})$$

$$\frac{dN_1}{dt} = -\beta N_1 \quad (\text{S-4})$$

The result of the differential equation could be shown as the following: $N_1 = N \exp(-\beta t)$, where N is the initial concentration of intermediates. So the probability of intermediates decay is:

$$P = \frac{N - N_1}{N} = \frac{N - N \exp(-\beta t)}{N} = 1 - \exp(-\beta t) \quad (\text{S-5})$$

Estimation of the distance between enzyme molecules in ZIF-8

In a typical experiment, we synthesized 0.0142 g of GOx/HRP@ZIF-8 composite. Since the density of ZIF-8 is 0.35 g/cm³, the volume of GOx/HRP@ZIF-8 composite was $4.061 \times 10^{-8} \text{ m}^3$. The SEM images of GOx/HRP@ZIF-8 composites clearly shown that the diameter of GOx/HRP@ZIF-8 particles was about 100 nm. Then we calculated the number of particles, with the result $N(\text{ZIF-8})=3.9 \times 10^{13}$. According to the amount of enzyme we added (GOx solution, 8 μL , 20 mg/mL and HRP solution 12 μL , 20 mg/mL), we get to know the number of enzyme molecules in GOx/HRP@ZIF-8 composite $N(\text{enzyme})=390 \times 10^{13}$. The calculations above determined the average number of enzyme molecules per GOx/HRP@ZIF-8 composite particle, which was 100. We randomly generated 100 points in a sphere with a diameter of 100 nm (**Figure S14**), and measured the distance between each point and the point closest to it, followed by averaging all the distances. Hence, the average distance between enzyme molecules in GOx/HRP_d10@ZIF-8 was $10.2 \pm 0.4 \text{ nm}$. With the same methods, we obtained the distances of enzyme molecules in GOx/HRP_d11@ZIF-8 and GOx/HRP_d13@ZIF-8 were $11.3 \pm 0.6 \text{ nm}$ and $13.1 \pm 0.8 \text{ nm}$, respectively.

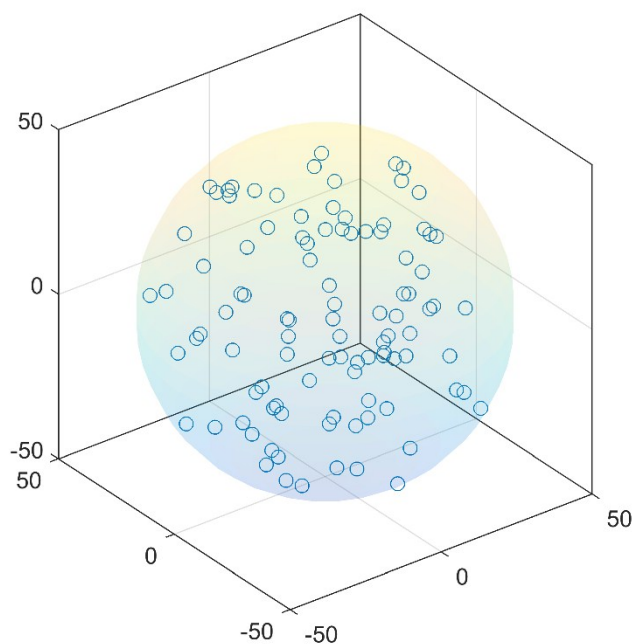


Figure S18. 100 points which were randomly generated in a sphere with a diameter of 100 *nm*

Materials

2-methylimidazole, zinc nitrate, glucose oxidase (GOx) from *Aspergillus niger*, horseradish peroxidase (HRP), catalase (CAT) from bovine liver and 2,2'-azino-bis(3-ethylbenzothiazoline-6-sulfonic acid) diammonium salt (ABTS), fluorescein isothiocyanate (FITC) were purchased from Sigma-Aldrich. Glucose and rhodamine B isothiocyanate (RhB) were purchased from Alfa Aesar.

Characterizations

High-angle annular dark-field scanning transmission electron microscopy (HAADF-STEM) and EDS mapping were recorded on a JEOL JEM-2100F instrument operated at 200 kV.

Scanning electron microscopy (SEM) images were taken on a Sirion 200 SEM at an accelerating voltage of 10 kV.

Transmission electron microscopy (TEM) images were taken on a JEOL JEM-2010 instrument working at 120 kV.

The powder X-ray diffraction (PXRD) patterns of GOx/HRP@ZIF-8 composites were characterized by a Bruker Advance D8 X-ray diffractometer with Cu K α ($\lambda = 1.5406 \text{ \AA}$) monochromatic radiation.

The absorbance of ABTS was determined on a UV/Vis spectrophotometer SHIMADZU UV-2600.

Laser scanning confocal microscopy images were taken on a Zeiss LSM 780 confocal microscope. The detection wavelengths were 488 nm for FITC and 543 nm for RhB.

Thermal gravimetric analysis (TGA) in nitrogen were performed on a TA instrument TGA 2050 Thermogravimetric Analyzer. The samples were heated from room temperature to 600 °C at a rate of 20 °C/min under nitrogen atmosphere.

Activity assay of GOx/HRP@ZIF-8 composite

Glucose (288 mg, 1.6 mmol), ABTS (5.48 mg) and GOx/HRP@ZIF-8 composites were added into the phosphate buffer solution (20 mL, 200 mM, pH 7.4), followed by stirring at room temperature and sampling periodically. For all the GOx/HRP@ZIF-8 samples, in the activity assay, the amounts of enzymes (containing 16 µg GOx and 24 µg HRP) were the same. After being centrifuged at 10 000 rpm for 1 min, the absorbance at 415 nm of supernatant was monitored on a Shimadzu UV-2600 UV-VIS Spectrophotometer.

To investigate the effect of intermediate decay on the overall activity of GOx/HRP@ZIF-8, CAT (10 µL, 2 mg/mL) was added into the above solution for activity assay.

Preparation of fluorescently labeled GOx/HRP@ZIF-8 composite

Dissolve fluorescein isothiocyanate (FITC) (2 mg) in DMSO (100 µL), add the mixture into GOx solution (1 mL, 10 mg/mL protein in 10 mM, pH 7.4 phosphate buffer solution). Then dissolve rhodamine B isothiocyanate (RhB) (2 mg), add the mixture into HRP solution (1 mL, 10 mg/mL protein in 10 mM, pH 7.4 phosphate buffer solution). The mixture was stirred in the dark at 4 °C overnight and followed by dialysis against phosphate buffer solution (10mM, pH 7.4) to remove free FITC and RhB. The fluorescent labeled FITC-GOx and RhB-HRP were used for the synthesis of GOx/HRP@ZIF-8 composites for laser scanning confocal microscopy characterization.

Table S1. The concentrations of GOx and HRP in the synthesis of GOx/HRP@ZIF-8 composites with different distances between GOx and HRP.

Sample	GOx [µg/mg ZIF-8]	HRP [µg/mg ZIF-8]	Embedding rate [%]
GOx/HRP_d10@ZIF-8	10	15	100
GOx/HRP_d11@ZIF-8	7.5	11.25	100
GOx/HRP_d13@ZIF-8	5	7.5	100
GOx/HRP_d15@ZIF-8	3.75	5.625	100
GOx/HRP_d17@ZIF-8	2.5	3.75	100

GOx/HRP_d23@ZIF-8	1.25	1.875	100
-------------------	------	-------	-----
